JSHC
Japan Society of Histochemistry and Cytochemistry
Established 1959

Acta Histochem. Cytochem. 40 (4): 101–111, 2007
doi:10.1267/ahc.07002

Review

Quantitative Colocalization Analysis of Multicolor Confocal Immunofluorescence Microscopy Images: Pushing Pixels to Explore Biological Phenomena

Vadim Zinchuk[1], Olga Zinchuk[2] and Teruhiko Okada[1]

[1]Department of Anatomy and Cell Biology, Kochi University Faculty of Medicine and [2]Department of Ophthalmology, Kochi University Faculty of Medicine, Okoh-cho, Nankoku, Kochi 783–8505, Japan

Received January 23, 2007; accepted June 8, 2007; published online August 2, 2007

Quantitative colocalization analysis is an advanced digital imaging tool to examine antigens of interest in immunofluorescence images obtained using confocal microscopes. It employs specialized algorithms to estimate the degree of overlap of fluorescence signals and thus enables acquiring important new information not otherwise obtainable using qualitative approaches alone. As raw confocal images have high levels of background, they should be prepared to become suitable for reliable calculation of colocalization coefficients by correcting it. We provide concise theoretical basis of quantitative colocalization analysis, discuss its limitations, and describe proper use of the technique. The use of quantitative colocalization analysis is demonstrated by studying bile salt export pump and multidrug resistance associated protein 2 in the liver and major basic protein and platelet activating factor receptor antigens in conjunctiva. The review is focused on the applicability and correct interpretation of the results of colocalization coefficients calculations.

Key words: confocal fluorescence microscopy, quantitative colocalization analysis, colocalization coefficients, colocalization software

I. Introduction

Colocalization of antigens is frequently observed by cell and molecular biologists studying them *in situ*. Antigens appear colocalized when immunohistochemical staining is performed to detect two or more antigens in the same section. Colocalization is detected by correspondent antibodies with different excitation spectra when staining of antigens visualized in different colors overlaps. Observation of colocalized antigens usually provides solid support for their common structural and functional characteristics [29, 30, 33].

The phenomenon of colocalization can be readily observed using images obtained with the help of confocal microscopes. These microscopes provide resolution required for viewing colocalization in images clearly. However, in the majority of cases it is not enough to only observe colocalization of studied antigens; significantly more important information can be obtained when estimating colocalization quantitatively. A number of recent reports employing quantitative colocalization analysis reflects a steadily growing interest to this tool [1, 2, 7, 13, 22, 24, 25, 32]. It is important that quantification of colocalization allows to follow the changes of its degree in dynamics and therefore information about degree of colocalization can considerably extend the applicability of qualitative observations [7, 33].

Proper use of quantitative colocalization analysis requires a certain degree of knowledge in the field, which is needed to avoid mistakes when using this tool [21]. Here, we summarize the knowledge needed to perform this analysis correctly. We review theoretical basis of quantitative colocalization and provide examples of its use. We also describe limitations of confocal images and give practical guidance on how the analysis should be carried out. The review is intended to serve as a concise guide for researchers performing quantitative colocalization analysis.

Correspondence to: Vadim Zinchuk, M.D., Ph.D., Department of Anatomy and Cell Biology, Kochi University Faculty of Medicine, Kohasu, Okoh-cho, Nankoku, Kochi 783–8505, Japan.
E-mail: zinchuk@s.kochi-u.ac.jp

II. What Is Colocalization?

Colocalization can be explained as an existence of the signal at the same pixel location when examining multi-channel fluorescence microscopy images. The channels are generated by two or more different fluorochromes when visualizing respective antigens and examining the same sample region. Although observation of colocalization of the antigens of interest itself does not provide direct proof of their functional relationship, it does give to researchers valuable clues regarding their structural and functional characteristics.

III. How Colocalization Analysis Is Performed

Colocalization is typically shown by presenting a plate of three images consisting of fluorescence for red and green channels, as well as a third merged image where the channels are combined and overlapping pixels turn yellow. It is crucial that the analysis includes exclusively antigens of interest and excludes any unspecific events generated by background and noise. The analysis is assisted by computer software. The software estimates the degree of colocalization according to specialized algorithms within the selected region of interest (ROI). The analysis is based on evaluation of color components of the selected pair of channels.

The proper assessment of colocalization requires background correction, i.e. defining the value of pixels intensity for the purpose of separating the features of interest from the rest of the image and then removing those pixels (see below). Quantitative colocalization analysis produces a number of coefficients for estimating the degree of colocalization (described in details below) as well as enables to view actual areas of colocalization on the images. The distribution of pixels according to channels can be viewed in two-dimensional scatter gram [5, 8]. Scatter gram represents information about image file and in itself is useful for the approximate estimation of the degree of colocalization in a given image [34] (Fig. 1). It can be embedded into the image to demonstrate its unique colocalization profile (Fig. 2).

IV. How Images with Colocalization should Be Acquired and Processed

Accurate estimation of colocalization depends on the quality of the images to be analyzed [5]. To obtain images of sufficient for the analysis quality [27], the following rules should be observed:

1. How to prepare colocalization sample:

a) Make sure that your chosen fluorophores have well-separated excitation and emission spectra.

b) Confirm specificity and the absence of cross-reaction of the used antibodies.

c) Do not change the mounting medium for your samples, as it may eventually change the level of background fluorescence.

d) Determine the level of autofluorescence by using unstained samples.

e) Use anti-fading reagents only if they are absolutely necessary.

2. How to properly set confocal microscope:

a) To avoid bleed-through effect, use optimized emission filters which help to maximize emission collection.

b) Remember to use plain chromatic lenses for reduction of chromatic shift.

c) Take care of the proper set up of the size of microscope pinhole.

d) Do not change objective lens when observing samples you plan to compare.

3. How to best acquire and handle images:

a) Avoid acquiring too bright and too high contrast images, as it will result in their saturation.

b) Do not acquire images simultaneously, use only sequential scanning. It will help to minimize the bleed-through effect.

c) When saving image using confocal microscope, choose TIFF graphics file format only (saving files in JPEG, PICT, BMP, etc. will result in loss of image data needed for

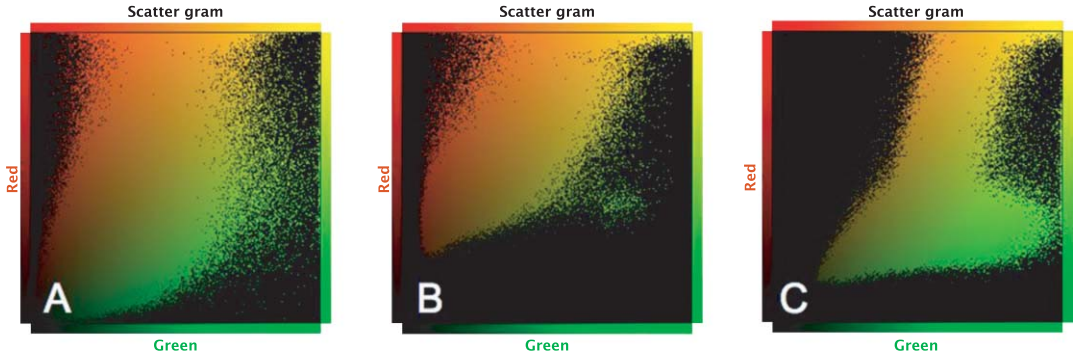

Fig. 1. Examples of scatter grams produced by colocalization analysis software and indicating differences of pixels distribution in analyzed images (**A–C**). Scatter grams show distribution of pixels in images according to selected pair of channels, in this case red-green. Colocalized yellow pixels are located along the diagonal. Note the split, "two-tailed" shape of scatter gram **C**. It shows the lowest percentage of colocalized pixels.

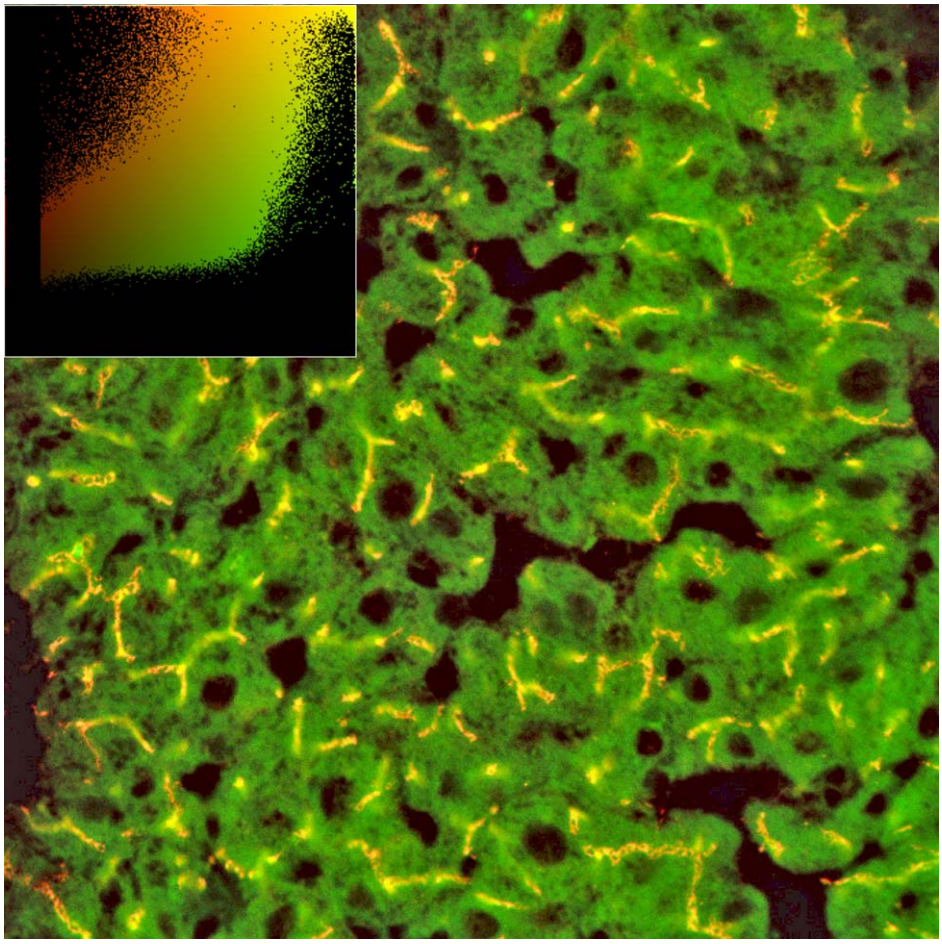

Fig. 2. Scatter gram of the analyzed image can be embedded into it to demonstrate its colocalization profile. Immunofluorescence of Mrp2 and Bsep proteins in the rat liver is shown on this image. An embedded scatter gram in upper left corner of the image estimates the amount of each detected antigen based on colocalization.

quantitation).

d) Avoid manipulation of your images in graphics-editing programs (Adobe Photoshop, GraphicConverter, etc.), as it may make them fully unusable for quantitation purposes.

V. Limitations of Confocal Images and Importance of Background Correction

It is important to remember that confocal images suffer from a high level of background noise [5]. This level can reach as much as 30% of maximum image intensity [16]. Thus, prior to performing measurements of colocalization, background of the images to be analyzed needs to be properly assessed and corrected. Erroneous background handling can complicate the reliability of a quantitative estimation of fluorescence imaging experiments. The extent of background correction depends on a variety of factors, including the intensity of immunofluorescence and the models of microscopes used to acquire images (Fig. 3). This step is highly critical and will impact the outcome of coefficients calculation. It should be pointed out that the latest colocalization software offers ready-to-use presets based on special algorithms for correcting background. These presets take into consideration the most common types of confocal images suffering from different levels of background and provide the possibility to correct background in one click. This approach also helps to ensure that all analyzed images were corrected exactly in the same way in one session and allows to re-use these settings in other sessions.

VI. Controlling Background Levels Using Filtering and Deconvolution

It should be noted that background can be partially suppressed using filtering and deconvolution [9, 26]. Filtering recovers a pixel value from surrounding areas and computes a weighted average. However, it results in loss of resolution as well as may result in artifacts. Deconvolution uses the imaging properties of the optical system in the form of point spread function for “putting the light back where it is coming from”. This technique improves background levels and produces more contrasted images. Drawbacks of deconvolution technique are as follows: 1) the need to exactly estimate the

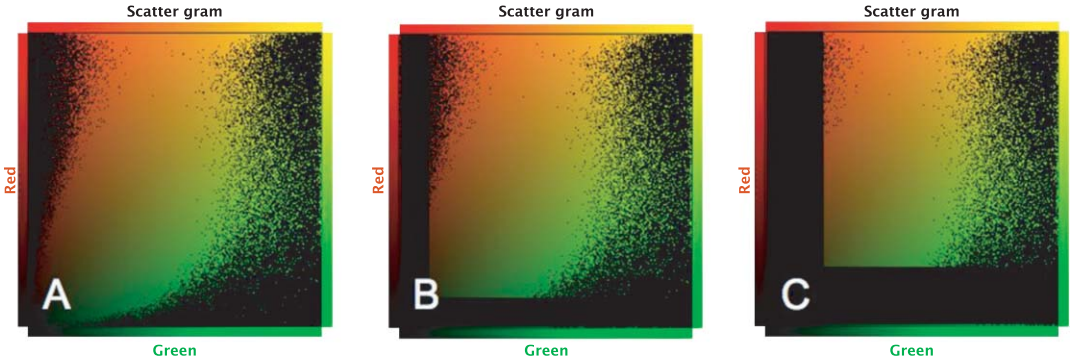

Fig. 3. Background correction removes pixels of certain levels and helps to ensure reliability of colocalization coefficients calculations. Examples of scatter grams produced by colocalization analysis software without (**A**) and with (**B, C**) corrected background. Black areas along X and Y axes in **B** and **C** indicate removed pixels. Scatter gram **C** has maximum pixels removed by background correction.

background and signal/noise ratio; 2) the need to employ very powerful computers; 3) the method is time consuming [16]. It needs to be mentioned that deconvolution technique should be used carefully, as it can introduce an unwanted bias, which may affect the colocalization results.

VII. Importance of Cross-talk Reduction

Another obstacle in obtaining reliable colocalization coefficients results is a cross-talk of fluorophores [4]. Cross-talk is a common problem when performing multiple fluorophore labeling experiments. High degree of cross-talk makes confocal images unusable for quantitative colocalization analysis. Though cross-talk can be hardly avoided completely, it can be significantly minimized by employing sequential laser scanning. Sequential scanning helps to minimize cross-talk between fluorophore channels by exciting each dye individually and then assembling obtained images into the final one [3, 10]. Although the latest models of confocal microscopes claim to provide a significantly improved cross-talk handling, it is still recommended to use sequential scanning for the images to be analyzed.

VIII. Coefficients Used to Estimate Colocalization

Colocalization is estimated using specially developed algorithms which calculate a number of respective coefficients, such as Pearson's correlation coefficient, overlap coefficient according to Manders, colocalization coefficients m1 and m2, colocalization coefficients M1 and M2, and overlap coefficients k1 and k2 [1, 19, 33, 34] were developed according to which colocalization can be evaluated quantitatively [5, 20]. These coefficients use different approaches to evaluate colocalization and have different sensitivity and applicability:

Pearson's correlation coefficient is one of the standard measures in pattern recognition:

$$R_r = \frac{\sum_i (S1_i - S1_{aver}) \cdot (S2_i - S2_{aver})}{\sqrt{\sum_i (S1_i - S1_{aver})^2 \cdot \sum_i (S2_i - S2_{aver})^2}}$$

where $S1$ represents signal intensity of pixels in the channel 1 and $S2$ represents signal intensity of pixels in the channel 2; $S1_{aver}$ and $S2_{aver}$ reflect the average intensities of these respective channels. It is used for describing the correlation of the intensity distributions between channels. It takes into consideration only similarity between shapes, while ignoring the intensities of signals. Its values range between −1.0 and 1.0, where 0 indicates no significant correlation and −1.0 indicates complete negative correlation. Negative values of Pearson's correlation coefficient, however, should be interpreted very cautiously. If you have obtained the values of this coefficient below 0, we recommend switching to Manders' overlap coefficient.

Overlap coefficient according to Manders indicates an overlap of the signals and thus represents the true degree of colocalization:

$$R = \frac{\sum_i S1_i \cdot S2_1}{\sqrt{\sum_i (S1_i)^2 \cdot \sum_i (S2_1)^2}}$$

where $S1$ represents signal intensity of pixels in the channel 1 and $S2$ represents signal intensity of pixels in the channel 2. This coefficient is not sensitive to the limitations of typical fluorescence imaging, such as efficiency of hybridization, sample photobleaching, and camera quantum efficiency. Its values are in the range from 0 to 1.0. If the image has overlap coefficient 0.5, it implies that 50% of both its objects, i.e. pixels, overlap. A value of zero means that there are no any overlapping pixels.

Colocalization coefficients m1 and m2 describe contribution of each one from two selected channels to the pixels of interest:

$$m_1 = \frac{\sum_i S1_{i,coloc}}{\sum_i S1_i}$$

$$m_2 = \frac{\sum_i S2_{i,coloc}}{\sum_i S2_i}$$

where $S1_{i,coloc} = S1_i$ if $S2_i > 0$ and $S2_{i,coloc} = S2_i$ if $S1_i > 0$. For example, if the red-green pair of channels is selected and m1 and m2 are 1.0 and 0.2, respectively, this means that all red pixels colocalize with green pixels, but only 20% of green pixels colocalize with red ones. The value of 1.0 for both channels indicates perfect colocalization.

Colocalization coefficients M1 and M2 are identical to m1 and m2, but applied to analyzing scatter gram ROI:

$$M1 = \frac{\sum_i S1_{i,coloc}}{\sum_i S1_i}$$

$$M2 = \frac{\sum_i S2_{i,coloc}}{\sum_i S2_i}$$

where $S1_{i,coloc} = S1_i$ if $S2_i > 0$ and $S2_{i,coloc} = S2_i$ if $S1_i > 0$, but, in contrast with m1 and m2 coefficeints, their applicability should be limited to the cases when scatter gram ROI is analyzed.

Overlap coefficients k1 and k2 split the value of colocalization into a pair of separate parameters:

$$k_1 = \frac{\sum_i S1_i \cdot S2_i}{\sum_i (S1_i)^2}$$

$$k_2 = \frac{\sum_i S1_i \cdot S2_i}{\sum_i (S2_i)^2}$$

where $S1$ represents signal intensity of pixels in the channel 1 and $S2$ represents signal intensity of pixels in the channel 2. They depend on the sum of the products of the intensities of two channels and are sensitive to the differences in the intensities of signals.

Summary of the comparison of these coefficients is given in Table 1. What coefficient to use depends on the images to be examined. In the majority of cases, Pearson's correlation coefficient provides clear and applicable results. However, if one antigen is stained stronger than another, then overlap coefficient according to Manders should be employed, as it allows to quantify colocalization coefficients in such images more reliably. Coefficients for the antigens on image with embedded scatter gram shown on Figure 2, for example, are as follows: Pearson's correlation coefficient=0.88, overlap coefficient according to Manders=0.92, colocalization coefficients m1 and m2=0.97 and 0.99, respectively, and overlap coefficients k1 and k2=1.24 and 0.68, respectively. These numbers suggest colocalization of bile salt export pump (Bsep) with multidrug resistance-

Table 1. *Brief comparison of coefficients used to estimate colocalization with their meanings, ranges of values, and use*

Coefficients	Meaning	Values	Use
Pearson's correlation coefficient [19].	Describes the correlation of the intensity distribution between channels [5, 20].	From –1.0 to 1.0; 0 indicates no significant correlation and –1.0 indicates complete negative correlation.	Can be used in any colocalization experiment.
Overlap coefficient according to Manders [19].	Indicates an actual overlap of the signals, represents the true degree of colocalization [5, 20].	From 0 to 1.0; 0.5 implies that 50% of both selected channels colocalize.	Can be used in any colocalization experiment, especially applicable when fluorescence of one antigen is stronger than of the other.
Colocalization coefficients m1 and m2 [34].	Describe contribution of each one from two selected channels to the pixels of interest [5, 20].	From 0 to 1.0; m1 and m2 of 1.0 and 0.2 for red-green pair imply that all red pixels colocalize with green, but only 20% of green pixels colocalize with red.	Can be used in any colocalization experiment.
Colocalization coefficients M1 and M2 [5, 20].	Identical to m1 and m2, but applied to analyze scatter gram ROI [5, 20].	From 0 to 1.0; m1 and m2 of 1.0 and 0.2 for red-green pair imply that all red pixels colocalize with green, but only 20% of green pixels colocalize with red.	Can be used in any colocalization experiment.
Overlap coefficients k1 and k2 [33].	Split the value of colocalization into the two separate parameters, allows to determine the contribution of each antigen to the areas with colocalization [5, 20].	Vary.	Can be used in any colocalization experiment.

associated protein 2 (Mrp2) proteins at the canalicular domain of the hepatocyte plasma membrane and justify results of previous observations [23, 35].

IX. Examples of Practical Use

Bile canalicular transporters

Colocalization of Mrp2 and Bsep proteins in the liver was studied following experimentally induced cholestasis [34]. Rats were injected intraperitoneally with either lipopolysaccharide (LPS) (2 mg/kg body weight) [28] or vehicle as a control. LPS from *Escherichia coli* 055:B5 (Difco Laboratories, Detroit, MI, USA) was dissolved in sterile physiological saline (0.9% NaCl, w/v). The animals were killed 2, 24, and 48 hr, and 1 week after injection. Livers were cut into pieces less than 1-mm thick, embedded in O.C.T. (Optimal Cutting Temperature) compound, and frozen in liquid nitrogen. Then, 8–10-µm-thick cryostat sections were picked up on glass slides, air-dried, and fixed in acetone. Bsep and Mrp2 antigens were examined using anti-Bsep (a generous gift of Dr. Bruno Stieger, Department of Medicine, University of Zurich, Switzerland) and anti-Mrp2 (goat) (Santa Cruz Biotechnology, Santa Cruz, CA, USA) antibodies, both diluted 1:100, for 1 hr. Sections were incubated with the mixture of corresponding secondary antibodies (conjugated with Alexa 488 and Alexa 594, respectively) (Molecular Probes, Eugene, OR, USA), diluted 1:400, for another 1 hr. In controls, primary antibodies were omitted from the labeling process. Sections were then examined using a confocal laser scanning microscope (CLSM) LSM 410 (Carl Zeiss, Jena, Germany). An immersion-oil Plan-Neofluar 40/0.75 objective was used. Double fluorescence for green and red channels was imaged using excitation of an argon-krypton laser at the wavelength of 488 and 543 nm. Double-stained images were obtained by sequential scanning for each channel to eliminate the "cross-talk" of chromophores and to ensure the reliable quantification of colocalization [8, 9]. Images were acquired and processed for colocalization analysis in TIFF format. Confocal images were then transferred to computer for analysis. Quantitative

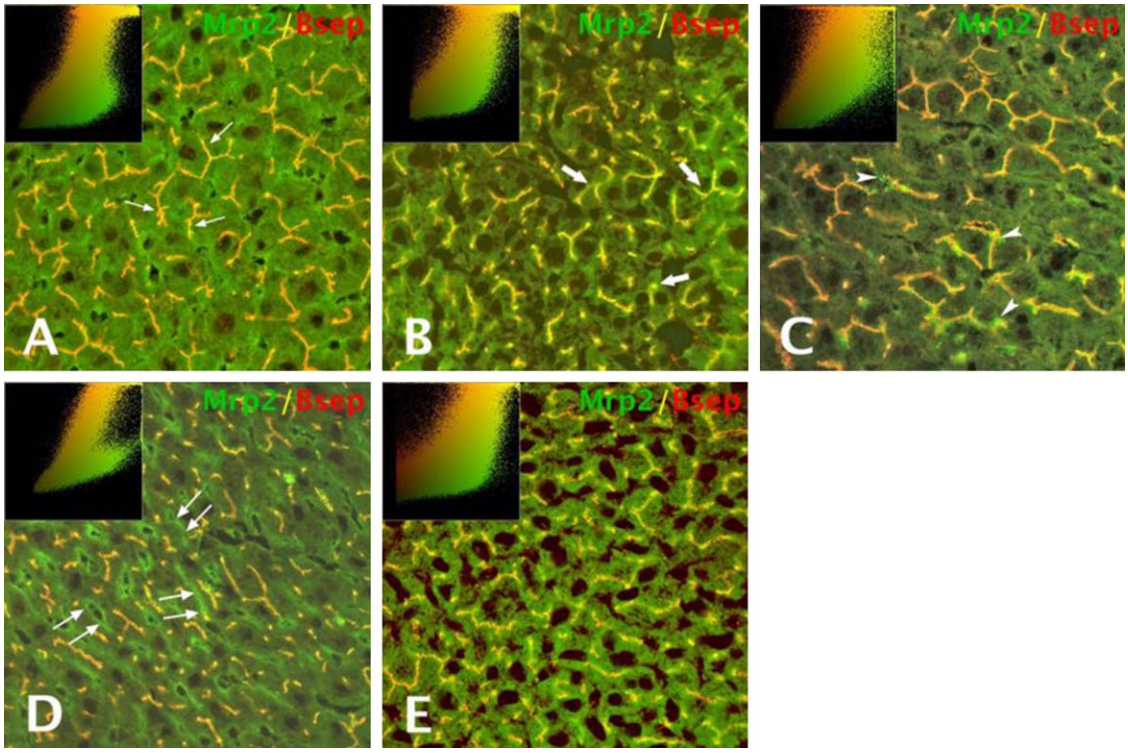

Fig. 4. Images showing immunofluorescence of Mrp2 (green) and Bsep (red) proteins in the liver (**A**) and changes of their colocalization pattern following LPS administration (**B–E**). Colocalization of Bsep and Mrp2 is revealed by the overlap of signals resulting in yellow staining. An embedded scatter gram estimates the amount of each detected antigens based on colocalization. Colocalized pixels of yellow color are located along the diagonal of scatter gram. The image of liver section of intact rats (**A**) reveals continuous staining of the bile canaliculi and precise colocalization of Mrp2 and Bsep antigens at them (arrows). The pattern of immunostaining changes 2 hr after injection of LPS (**B**), with the appearance of fuzzy-looking areas of fluorescence of both proteins and weaker delineated canaliculi (thick arrows). At 24 hr, the pattern of immunostaining changes further (**C**). Note dots of immunofluorescence of both proteins in subapical areas of hepatocytes (arrowheads). At 48 hr (**D**), in addition to canaliculi, immunostaining of Mrp2 appears at the basolateral domain of hepatocytes as well (double arrows). The split, "two-tailed" nature of the scatter gram is most pronounced at the time when colocalization coefficients show the lowest numbers (**D**). By 1 week, sections reveal immunostaining resembling that seen in intact animals (**E**). Magnification=×400.

analysis was performed employing CoLocalizer Pro of CoLocalization Research Software. Background was corrected in Auto mode by selecting image pattern preset at "Average Contrast and Fluorescence". ROIs were selected using lasso tool to include as minimum areas without fluorescence as possible. Pearson's correlation coefficient (PCC), an overlap coefficient according to Manders (MOC), and overlap coefficients k1 and k2 were examined.

Mrp2 and Bsep proteins were detected in intact animals exclusively at the bile canaliculi and colocalized (Fig. 4A). This observation of colocalization was supported by the results of coefficients calculations: PCC was 0.996, while MOC was 0.992 (Fig. 5A, B). LPS administration resulted in the appearance of fuzzy-looking areas of fluorescence of Mrp2 and Bsep proteins around bile canaliculi 2 hr after injection (Fig. 4B). Then, by 24 hr, immunofluorescence for both proteins had become detectable in subapical areas of hepatocytes (Fig. 4C). At 48 hr, in addition to canaliculi, immunostaining of Mrp2 appeared at the basolateral domain of hepatocytes as well (Fig. 4D). By 1 week, sections revealed immunostaining resembling that seen in intact animals (Fig. 4E). PCC decreased after exposure to LPS reaching its lowest level at 48 hr after injection (0.712) and then recovered by 1 week to 0.887 (Fig. 5A). Similarly, MOC decreased and reached 0.685 at 48 hr and by 1 week recovered to 0.717 (Fig. 5B). Therefore, the changes of morphological distribution of Mrp2 and Bsep proteins were in agreement with the results of PCC and MOC coefficients calculations.

It should be noted that calculation of PCC and MOC showed significant decrease of their numbers as compared to controls, which can not be explained merely by relocation of Mrp2 protein toward the basolateral membrane. These results revealed a more complex mechanism of the reaction of Bsep and Mrp2 to LPS challenge that can be envisioned evaluating images qualitatively only. The complexity of this reaction was supported by the results of calculation of overlap coefficients k1 and k2 too. These coefficients showed different contribution to colocalization of Mrp2 and Bsep proteins in intact and experimental animals. In intact rats, Mrp2 contributed to colocalization with Bsep more (1.24 for Mrp2 and 0.75 for Bsep) than Mrp2. Their contribution was equal at 24 hr after LPS administration. By 1 week, Mrp2 and Bsep proteins changed their roles, i.e., contribution of Mrp2 was 0.78, while contribution of Bsep was 1.21 (Fig. 5C). Thus, the results of coefficients calculations helped to find out more about the mechanism of involvement of Bsep and Mrp2 proteins in hepatocytes following LPS administration than it was possible to do using morphological experiments only.

Eosinophils in conjunctiva

Colocalization analysis has been employed to quantify the degree of colocalization of major basic protein (MBP) and platelet activating factor receptor (PAF-R) antigens on eosinophils in the course of PAF-induced conjunctivitis [33]. Male Brown Norway rats were used in this experiment. Eyes were challenged with 1% solution of PAF. PAF was

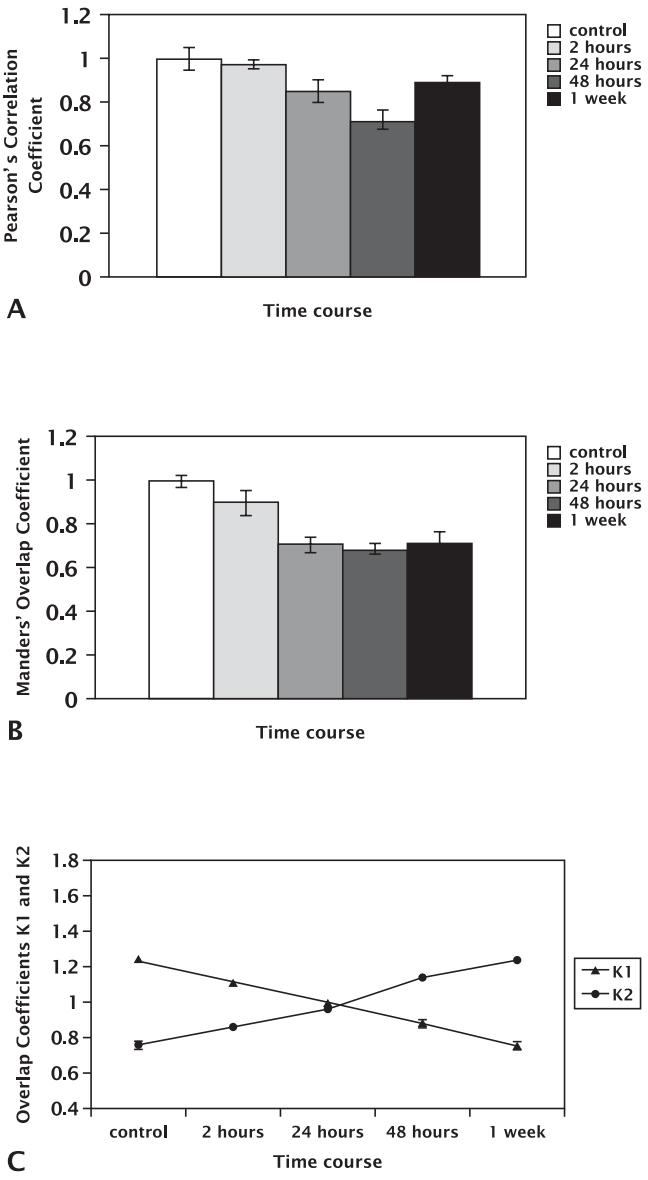

Fig. 5. Changes of Pearson's correlation coefficient (PCC) (**A**), overlap coefficient according to Manders (MOC) (**B**), and overlap coefficients k1 and k2 (**C**) following LPS administration. PCC shows its lowest level at 48 hr. By 1 week, it restores its value, although does not reach the control levels. MOC shows a steady decrease of the degree of colocalization of Mrp2 and Bsep proteins. The speed of decrease slows at 48 hr, where it reaches its lowest level, then slightly increases by 1 week. K1 and k2 coefficients indicate the contribution of Bsep and Mrp2 proteins to the process colocalization. In the intact animals, Bsep contributes to the colocalization more than Mrp2. By one week, they change roles. CoLocalizer Pro software was used to calculate colocalization coefficients. An average of coefficients of three examined samples for each time point is shown. $P<0.05$. Error bars indicate standard deviation.

purchased either from Cayman (Cayman Chemical, Ann Arbor, MI, USA) or from Alexis Biochemicals (Tokyo, Japan) and prepared according to the manufacturer's recommendations. Eyes were collected 30 min, 2, 6, and 24 hr following PAF instillations. In controls, PBS was used instead of PAF solution. Eyes were harvested with intact conjunctivas. Sections (6 µm thick) were cut using a cryomicrotome. After fixation, sections were incubated with anti-PAF-receptor (Cayman Chemical, Ann Arbor, MI, USA) and anti-major basic protein (MBP; Biodesign International, Saco, ME, USA) primary antibodies. Sections were then exposed to the corresponding secondary antibodies (conjugated with Alexa 488 and Alexa 594; Molecular Probes, Eugene, OR, USA), diluted 1:400. In controls, primary antibodies were omitted from the labeling process. Confocal immunofluorescence microscopy and quantitative colocalization analysis were performed as described above. Background was corrected using the threshold value for all channels to remove background and noise levels completely. PCC, MOC, and overlap coefficients k1 and k2 were examined.

Confocal immunofluorescence microscopy showed the expression of PAF-R on eosinophils in all examined samples and at all time points, including controls, indicating the presence of PAF-R on eosinophils even in the intact state (Fig. 6A). Quantitative colocalization analysis demonstrated high degree of colocalization even in controls (Fig. 7C). Eventually, it showed a gradual increase as the PAF-induced inflammation developed. In intact animals, PCC was 0.890, MOC was 0.886. At 30 min after PAF administration, PCC was 0.901, MOC was 0.899, and at 2, 6, 24 hr the coefficients were: 0.945, 0.939, 0.973, and 0.972, 0.992, 0.995 respectively. It is important to note, that the two coefficients, namely PCC and MOC, while revealing the different aspects of the colocalization process, showed similar pattern of changes, proving the applicability of the calculations to investigate the degree of colocalization of antigens.

Interestingly, when the number of infiltrating eosinophils started to decrease (Fig. 7A) and clinical signs of the inflammatory reaction almost vanished (by 24 hr after PAF administration), the number of PAF-R positive cells (Fig. 7B) and the degree of colocalization (Fig. 7C) still kept increasing. These findings might indicate that eosinophils found in the conjunctiva sections at this time point maintained an elevated expression of PAF-R. On the other hand, they might reflect the changes of the expression of PAF-R antigen by other cells. Calculation of two more colocalization coefficients, K1 and K2, has helped to shed the light on these questions. It was found that the degree of PAF-R expression was gradually increasing during our experiment (in control animals, coefficient K1, reflecting the impact of PAF-R antigen, was 0.857, 30 min after PAF instillation, it was 0.905, at 2, 6, 24 hr it was 0.934, 0.994 and 1.048 re-

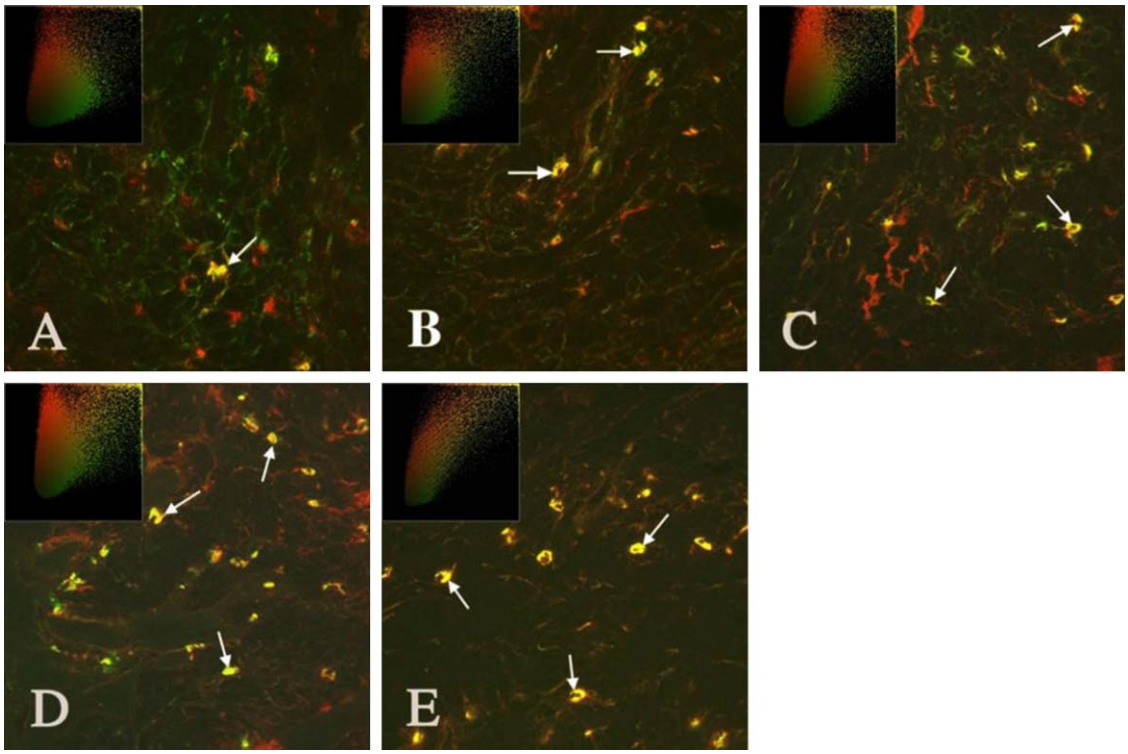

Fig. 6. Confocal immunofluorescence microscopy of conjunctiva sections stained with anti-PAF-R (red fluorescence) and anti-MBP (green fluorescence) antibodies. Embedded scatter gram in the upper left corner of the image estimates the amount of each detected antigen based on colocalization of PAF-R (red, y-axis) and MBP (green, x-axis). Colocalized pixels of yellow color are located along the diagonal of the scatter gram. All shown images reveal colocalization of PAF-R and MBP antigens at different time points (arrows) (**A–E**). See text for details. Magnification=×400.

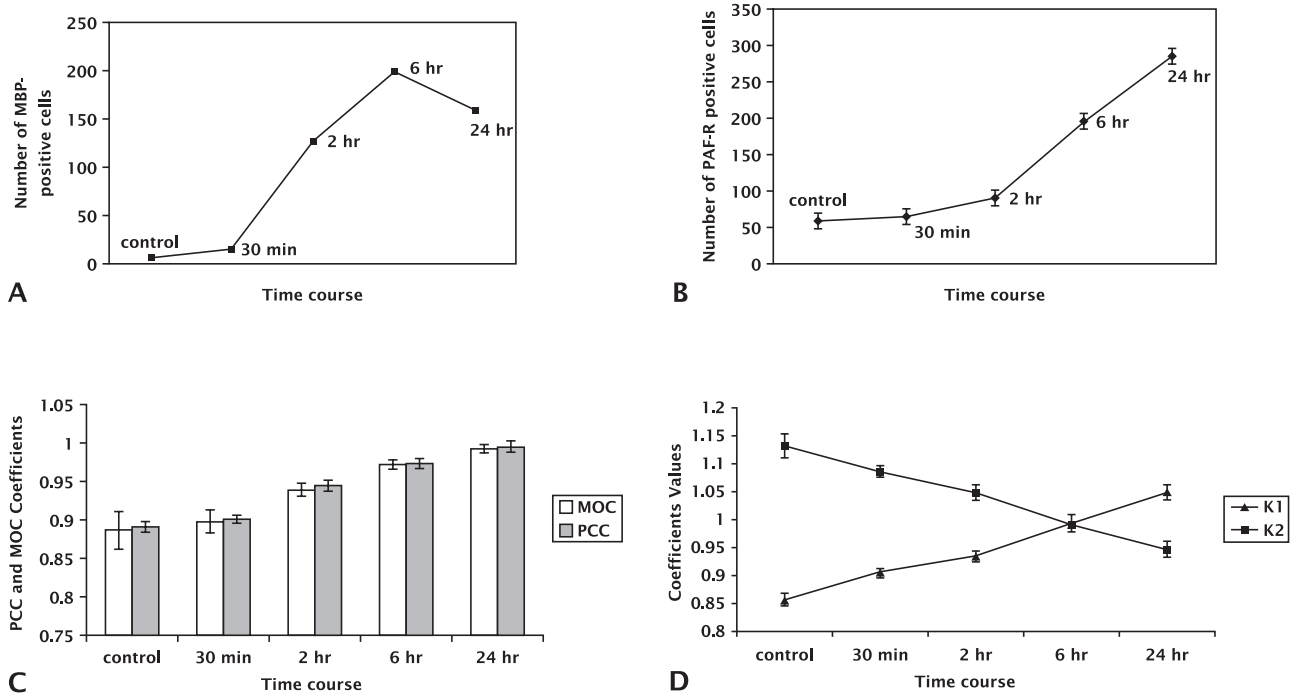

Fig. 7. Dynamical changes of the expression of antigens. Dynamical changes of MBP expression as a time course of the changes of the number of MBP-positive cells are presented (**A**). An average of the data of three examined samples for each time point is presented. P<0.05. Time course of the changes of the number of immuno-positive cells demonstrates the dynamical changes of PAF-R expression in the conjunctiva (**B**). An average data of three examined samples for each time point is presented. P<0.05. Overlap coefficient K1, reflecting the impact of PAF-R antigen, shows that the degree of PAF-R expression increases during the course of PAF-induced conjunctivitis. The impact of MBP antigen to the process of colocalization reflected by the K2 overlap coefficient decreases by 24 hr after PAF administration (**C**). An average data of three examined samples for each time point is presented. P<0.05. Quantitative analysis shows a steady increase of the degree of colocalization as a result of PAF administration (**D**). CoLocalizer Pro software was used to calculate colocalization coefficients. An average of MOC and PCC of three examined samples for each time point is shown. P<0.05.

spectively), while expression of MBP antigen decreased (K2 coefficient, reflecting the impact of MBP antigen to the process of colocalization, was 1.131 in the intact animals, at 30 min, 2, 6, and 24 hr K2 was 1.087, 1.049, 0.992 and 0.947, respectively) (Fig. 7D). These data gave the reason to conclude that administration of PAF caused a further increase of the degree of PAF-R expression by eosinophils even when the severity of inflammatory reaction was fading. Interestingly, the peak of the number of infiltrating eosinophils detected using histological examination coincided with the moment, at 6 hr after PAF administration (Fig. 4A), when K1 equaled K2 (Fig. 7D), i.e., when the intensities of MBP and PAF-R antigen signals were the same. After this period of time, the K1 continued to grow, but the number of infiltrating eosinophils was no longer increasing. This might imply that the interaction of both PAF-R and MBP antigens with PAF is required for the recruitment of eosinophils. Quantitative colocalization analysis helped to determine that the recruitment of eosinophils in PAF-induced conjunctivitis is accomplished via direct action of PAF toward the PAF-R. These findings and other important conclusions would have been impossible to make without performing quantification of colocalization of MBP and PAF-R antigens.

X. Future Perspectives

Utility of quantitative colocalization analysis is supported by the constant improvement of the quality of images produced by confocal microscopes and by the introduction of various image-processing techniques, which enhance signal-to-noise ratio and improve suitability of images for this analysis [15]. In addition, new algorithms for estimating colocalization have been introduced [6, 31]. Algorithm developed by Costes *et al.* (2004) introduced a novel statistical approach that quantifies the amount of colocalization in an image quantitatively, removing the basis for visual interpretation. This algorithm can be applied to study colocalization on three-dimensional (3D) sets of cells. It remains to be seen whether this new algorithm will be adopted and whether it will bring further improvements to this important technique. Other complex approaches using automated image analysis for 3D quantification have the potential to be applied for quantitative colocalization analysis as well [17]. It should be noted that newly developed algorithms attempt to consider various important factors, such as the ratio of intensity of fluorescence of individual fluorophores, the effect of fluorescence fading, and even the number of times the section

Table 2. *Steps of quantitative colocalization analysis*

1. Image acquisition	Images should be obtained using sequential scanning for each channel to eliminate the "cross-talk" of chromophores and to ensure the reliable quantification of colocalization and saved in TIFF format to prevent the loss of information.
2. Background correction	A. The extent of background correction depends on a variety of factors, including the intensity of immunofluorescence and the models of microscopes used to acquire images. B. For the results to be comparable, background correction settings should be the same for all images in a study.
3. Coefficients calculations	Several algorithms, such as Pearson's correlation coefficient, overlap coefficient according to Manders, colocalization coefficients m1 and m2, colocalization coefficients M1 and M2, and overlap coefficients k1 and k2 use different approaches to estimate colocalization and have different sensitivity and applicability. What coefficient to use depends on the images to be examined. In majority of cases, Pearson's correlation coefficient provides clear and applicable results. However, if one antigen is stained stronger than another, then overlap coefficient according to Manders should be employed, as it allows to quantify colocalization coefficients in these images more reliably.
4. Interpreting obtained results	A. Pearson's correlation coefficient—correlation of the intensity distribution between channels. B. Overlap coefficient according to Manders—the true degree of colocalization. C. Overlap and colocalization coefficients—contribution of each particular antigen to the areas with colocalization.

was scanned prior to saving the image of interest [12]. When applied to quantitative colocalization analysis, these algorithms should be capable of producing more accurate and reproducible coefficients results. Another new and exceptionally promising trend in quantitative colocalization analysis is single-molecule colocalization in living cells [11, 14, 18]. Although this technique requires improvements of signal/noise and signal/background ratios, it offers a more robust measure of colocalization and can produce more applicable results.

XI. Conclusion

We used quantitative colocalization analysis to demonstrate changes of localization of Bsep and Mrp 2 antigens in liver and MBP and PAF-R antigens in conjunctiva using confocal microscopy images and characterized their dynamics in experimentally induced cholestasis and in the course of PAF-induced conjunctivitis, respectively. The use of quantitative colocalization allowed to objectively compare changes of colocalization of the antigens of interest. It also allowed to measure the contribution of each particular antigen to the process of colocalization and to compare the extent of their contribution. The use of advanced computer software made quantitative colocalization analysis an automated and easily reproducible procedure.

The following should be remembered and strictly adhered to for proper execution of quantitative colocalization analysis: 1) Images should be obtained by sequential scanning for each channel to eliminate the cross-talk of chromophores and to ensure the reliable quantification of colocalization and then saved in TIFF format to prevent the loss of information. 2) Images should have their background corrected by removing pixels of unwanted levels. For the results to be comparable, background correction settings should be the same for all images in a study. 3) The most applicable coefficients are Pearson's correlation coefficient and overlap coefficient according to Manders. 4) Colocalization coefficients results should be applied depending on the analyzed images and interpreted strictly within the range of their corresponding values. This information is summarized in Table 2.

XII. Conflict of Interests Statement

The authors declare no conflict of interests.

XIII. References

1. Agnati, L. F., Fuxe, K., Torvinen, M., Genedani, S., Franco, R., Watson, S., Nussdorfer, G. G., Leo, G. and Guidolin, D. (2005) New methods to evaluate colocalization of fluorophores in immunocytochemical preparations as exemplified by a study on A2A and D2 receptors in Chinese hamster ovary cells. *J. Histochem. Cytochem.* 53; 941–953.
2. Cario, E., Golenbock, D. T., Visintin, A., Runzi, M., Gerken, G. and Podolsky, D. K. (2006) Trypsin-sensitive modulation of intestinal epithelial MD-2 as mechanism of lipopolysaccharide tolerance. *J. Immunol.* 176; 4258–4266.
3. Carlsson, K., Aslund, N., Mossberg, K. and Philip, J. (1994) Simultaneous confocal recording of multiple fluorescent labels with improved channel separation. *J. Microsc.* 176; 287–299.
4. Carlsson, K. and Ulfhake, B. (1995) Improved fluorophore separation with IMS confocal microscopy. *Neuroreport* 6; 1169–1173.
5. CoLocalization Research Software, I. (2006) CoLocalizer Pro User Guide. CoLocalization Research Software, Inc. Ver. 2.
6. Costes, S. V., Daelemans, D., Cho, E. H., Dobbin, Z., Pavlakis, G. and Lockett, S. (2004) Automatic and quantitative measurement of protein-protein colocalization in live cells. *Biophys. J.* 86; 3993–4003.
7. Criscuoli, M. L., Nguyen, M. and Eliceiri, B. P. (2005) Tumor metastasis but not tumor growth is dependent on Src-mediated vascular permeability. *Blood* 105; 1508–1514.

8. Demandolx, D. and Davoust, J. (1995) Multicolor analysis in confocal immunofluorescence microscopy. *J. Trace Microprobe Tech.* 13; 217–225.
9. Demandolx, D. and Davoust, J. (1997) Multicolour analysis and local image correlation in confocal microscopy. *J. Microsc.* 185; 21–36.
10. Foldes-Papp, Z. (2005) How the molecule number is correctly quantified in two-color fluorescence cross-correlation spectroscopy: corrections for cross-talk and quenching in experiments. *Curr. Pharm. Biotech.* 6; 437–444.
11. Fujiwara, T., Ritchie, K., Murakoshi, H., Jacobson, K. and Kusumi, A. (2002) Phospholipids undergo hop diffusion in compartmentalized cell membrane. *J. Cell Biol.* 157; 1071–1081.
12. Jaskolski, F., Mulle, C. and Manzoni, O. J. (2005) An automated method to quantify and visualize colocalized fluorescent signals. *J. Neurosci. Methods* 146; 42–49.
13. Kato, T., Muraski, J., Chen, Y., Tsujita, Y., Wall, J., Glembotski, C. C., Schaefer, E., Beckerle, M. and Sussman, M. A. (2005) Atrial natriuretic peptide promotes cardiomyocyte survival by cGMP-dependent nuclear accumulation of zyxin and Akt. *J. Clin. Invest.* 115; 2716–2730.
14. Koyama-Honda, I., Ritchie, K., Fujiwara, T., Iino, R., Murakoshi, H., Kasai, R. S. and Kusumi, A. (2005) Fluorescence imaging for monitoring the colocalization of two single molecules in living cells. *Biophys. J.* 88; 2126–2136.
15. Landmann, L. (2002) Deconvolution improves colocalization analysis of multiple fluorochromes in 3D confocal data sets more than filtering techniques. *J. Microsc.* 208; 134–147.
16. Landmann, L. and Marbet, P. (2004) Colocalization analysis yields superior results after image restoration. *Microsc. Res. Tech.* 64; 103–112.
17. Lin, G., Bjornsson, C. S., Smith, K. L., Abdul-Karim, M. A., Turner, J. N., Shain, W. and Roysam, B. (2005) Automated image analysis methods for 3-D quantification of the neurovascular unit from multichannel confocal microscope images. *Cytometry* 66; 9–23.
18. Lommerse, P. H., Blab, G. A., Cognet, L., Harms, G. S., Snaar-Jagalska, B. E., Spaink, H. P. and Schmidt, T. (2004) Single-molecule imaging of the H-ras membrane-anchor reveals domains in the cytoplasmic leaflet of the cell membrane. *Biophys. J.* 86; 609–616.
19. Manders, E. M. M., Verbeek, F. J. and Aten, J. A. (1993) Measurement of co-localization of objects in dual-colour confocal images. *J. Microsc.* 169; 375–382.
20. Media Cybernetics, I. (2002) Image-Pro Plus Application Note #1: Colocalization of fluorescent probes.
21. North, A. J. (2006) Seeing is believing? A beginners' guide to practical pitfalls in image acquisition. *J. Cell Biol.* 172; 9–18.
22. Patel, H. H., Head, B. P., Petersen, H. N., Niesman, I. R., Huang, D., Gross, G. J., Insel, P. A. and Roth, D. M. (2006) Protection of adult rat cardiac myocytes from ischemic cell death: role of caveolar microdomains and delta-opioid receptors. *Am. J. Physiol. Heart Circ. Physiol.* 291; H344–350.
23. Paulusma, C. C., Kothe, M. J., Bakker, C. T., Bosma, P. J., van Bokhoven, I., van Marle, J., Bolder, U., Tytgat, G. N. and Oude Elferink, R. P. (2000) Zonal down-regulation and redistribution of the multidrug resistance protein 2 during bile duct ligation in rat liver. *Hepatology* 31; 684–693.
24. Petrescu, A. D., Payne, H. R., Boedecker, A., Chao, H., Hertz, R., Bar-Tana, J., Schroeder, F. and Kier, A. B. (2003) Physical and functional interaction of Acyl-CoA-binding protein with hepatocyte nuclear factor-4 alpha. *J. Biol. Chem.* 278; 51813–51824.
25. Scriven, D. R., Klimek, A., Asghari, P., Bellve, K. and Moore, E. D. (2005) Caveolin-3 is adjacent to a group of extradyadic ryanodine receptors. *Biophys. J.* 89; 1893–1901.
26. Shaw, P. and Rawlins, D. J. (1991) The point spread function of confocal microscope: its measurement and use in deconvolution. *J. Microsc.* 163; 151–165.
27. Smallcombe, A. (2001) Multicolor imaging: the important question of co-localization. *BioTechniques* 30; 1240–1242, 1244–1246.
28. Spolarics, Z., Stein, D. S. and Garcia, Z. C. (1996) Endotoxin stimulates hydrogen peroxide detoxifying activity in rat hepatic endothelial cells. *Hepatology* 24; 691–696.
29. Swaney, J. S., Patel, H. H., Yokoyama, U., Head, B. P., Roth, D. M. and Insel, P. A. (2006) Focal adhesions in (myo)fibroblasts scaffold adenylyl cyclase with phosphorylated caveolin. *J. Biol. Chem.* 281; 17173–17179.
30. Tsutsumi, Y. M., Patel, H. H., Huang, D. and Roth, D. M. (2006) Role of 12-lipoxygenase in volatile anesthetic-induced delayed preconditioning in mice. *Am. J. Physiol. Heart Circ. Physiol.* 291; H979–983.
31. Wouters, F. S., Verveer, P. J. and Bastiaens, P. I. (2001) Imaging biochemistry inside cells. *Trends Cell Biol.* 11; 203–211.
32. Zinchuk, O., Fukushima, A. and Hangstefer, E. (2004) Dynamics of PAF-induced conjunctivitis reveals differential expression of PAF receptor by macrophages and eosinophils in the rat. *Cell Tissue Res.* 317; 265–277.
33. Zinchuk, O., Fukushima, A., Zinchuk, V., Fukata, K. and Ueno, H. (2005) Direct action of platelet activating factor (PAF) induces eosinophil accumulation and enhances expression of PAF receptors in conjunctivitis. *Mol. Vis.* 11; 114–123.
34. Zinchuk, V., Zinchuk, O. and Okada, T. (2005) Experimental LPS-induced cholestasis alters subcellular distribution and affects colocalization of Mrp2 and Bsep proteins: a quantitative colocalization study. *Microsc. Res. Tech.* 67; 65–70.
35. Zinchuk, V. S., Okada, T., Akimaru, K. and Seguchi, H. (2002) Asynchronous expression and colocalization of Bsep and Mrp2 during development of rat liver. Am. J. Physiol. Gastrointest. Liver Physiol. 282; G540–548.